

Profiling B cell chronic lymphocytic leukemia by reverse phase protein array: Focus on apoptotic proteins

Federica Frezzato,^{*,†} Benedetta Accordi,[‡] Valentina Trimarco,^{*,†} Cristina Gattazzo,^{*,†}
Veronica Martini,^{*,†} Gloria Milani,[‡] Silvia Bresolin,[‡] Filippo Severin,^{*,†} Andrea Visentin,^{*,†}
Giuseppe Basso,[‡] Gianpietro Semenzato,^{*,†,1} and Livio Trentin^{*,†,2}

^{*}Department of Medicine, Hematology and Clinical Immunology Branch, Padua University School of Medicine, Padova, Italy;

[†]Venetian Institute of Molecular Medicine, Padova, Italy; and [‡]Department of Women's and Children's Health, University of Padua, Padova, Italy

RECEIVED JULY 15, 2015; REVISED APRIL 26, 2016; ACCEPTED MAY 17, 2016. DOI: 10.1189/jlb.2AB0715-301R

ABSTRACT

B cell chronic lymphocytic leukemia (CLL) is characterized by the accumulation of B lymphocytes from proliferative activity and apoptosis resistance. The increased awareness of the importance of B cell receptor signaling in CLL has raised new opportunities for targeted intervention. Herein, we describe a study performed with the high-throughput RPPA (reverse phase protein array) technique, which allowed us to simultaneously study different molecules in a large series of patients. We analyzed B lymphocytes from 57 patients with CLL and 11 healthy subjects. Different pathways were assessed for activation/expression of key signaling proteins. Data obtained were validated by Western blotting and confocal microscopy. The RPPA investigation and its validation, identified 3 series of proteins: 1) molecules whose expression levels reached statistically significant differences in CLL vs. healthy controls (HSP70, Smac/DIABLO, cleaved PARP, and cleaved caspase-6); 2) proteins with a positive trend of difference in CLL vs. healthy controls (HS1, γ -tubulin, PKC α/β -II Thr-638/641, p38 MAPK Thr-180/Tyr-182, NF- κ B Ser-536, Bcl2 Ser-70 and Src Tyr-527); and 3) molecules differentially expressed in patients with IGHV mutations vs. those without mutations (ZAP70, PKC- ζ λ , Thr-410/403, and CD45). This study identified some molecules, particularly those involved in apoptosis control, which could be considered for further studies to design new therapeutic strategies in CLL. *J. Leukoc. Biol.* 100: 1061-1070; 2016.

Introduction

CLL is a neoplastic disease characterized by the accumulation of clonal B cells from uncontrolled growth and resistance to apoptosis [1]. The pathogenic mechanisms of CLL involve

both intrinsic (unbalanced proliferation/apoptosis and impaired signal transduction mediated by the BCR) and extrinsic (microenvironment) events, crucial for the transformation and growth of CLL cells as well as for the progression of the disease [2]. Prognostic factors, in particular, the mutational status of the IGHV genes, divide patients with CLL into those with good vs. poor prognosis [3]. Most patients present with relatively indolent disease, which enables detailed investigation of their tumor cells as well as observations of the tumor behavior over time. This opportunity allowed the identification of prognostic factors related to CLL pathogenesis. However, despite innovative prognostic markers and therapies for this disease, which have improved the clinical outcome, CLL remains incurable. Therefore, researchers must identify specific targets to develop new therapeutic strategies against the disease.

The purpose of this study was to gain information about the CLL proteome with the RPPA technology [4] to identify new proteins or signaling pathways that might contribute to the pathogenesis of this disease, with the final goal of defining specific targets for the development of new therapeutic strategies.

The BCR pathway, crucial in CLL physiopathology, is currently the target of innovative therapies being tested in several clinical trials, with the most promising results being generated by Btk and PI3K- δ inhibitors. Ongoing multicenter studies also include the use of Lyn, Lck, Syk, and ZAP70 inhibitors [5].

MATERIALS AND METHODS

Patients, cell separation, and culture conditions

B cell samples were collected from 57 therapy-free patients with CLL who satisfied standard morphologic and immunophenotypic criteria for CLL cells.

Abbreviations: BH = Benjamini-Hochberg, CLL = chronic lymphocytic leukemia, HSP70 = heat shock protein of 70 kDa, IGHV = immunoglobulin heavy chain variable region, PARP = poly(ADP-ribose) polymerase, RPPA = reverse phase protein array, SFK = src family kinase, WB = Western blotting

1. Correspondence: Department of Medicine, University of Padova, Via Giustiniani 2, 35128-Padova, Italy. E-mail: g.semenzato@unipd.it
2. Correspondence: Department of Medicine, University of Padova, Via Giustiniani 2, 35128-Padova, Italy. E-mail: livio.trentin@unipd.it

Informed consent was obtained from all patients according to the Declaration of Helsinki. Patient characteristics are reported in **Table 1**. All specimens, collected at the Hematology and Clinical Immunology Branch, Padova University School of Medicine, from 2003 to 2008, were snap-frozen in DMSO in liquid nitrogen. PBMCs were obtained by Ficoll gradient centrifugation (GE Healthcare, Little Chalfont, United Kingdom). When necessary, B cells were purified from the PBMCs by removing T cells with the sheep erythrocyte rosetting method. The samples that were used had $\geq 95\%$ CD19⁺/CD5⁺ cells, as assessed by flow cytometry. Untouched, peripheral-blood B cells were isolated from the PBMCs of 11 healthy donors by negative selection with the RosetteSep for isolation of B cells (StemCell Technologies, Vancouver, BC, Canada). The purity of the healthy B cells obtained was $\geq 95\%$ (CD19⁺) as assessed by flow cytometry. At the time of the experiments, frozen samples were defrosted and washed 2 times with RPMI 1640 medium supplemented with 10% heated-inactivated FCS (Thermo Fisher Scientific, Waltham, MA, USA). After thawing, cell viability was assessed by flow cytometry, and all the samples had $\geq 85\%$ living cells. To study HSP70, we used B cells obtained from 6 patients with CLL before and after therapy with R-FC or R-benda. For experiments on HSP70 inhibition, we used pifithrin- μ (Selleckchem, Houston, TX, USA) at 5, 10, and 15 μ M for 24-h incubation.

Protein extraction for RPPA

After sample collection, cells were lysed in a buffer containing T-PER reagent (Thermo Fisher Scientific), NaCl (5 M), sodium orthovanadate (1 mM), Pefabloc SC (200 mM AEBSF; Roche Diagnostics, Indianapolis, IN, USA), aprotinin (5 mg/ml), pepstatin A (1 mg/ml), and leupeptin (5 mg/ml; Sigma-Aldrich, St. Louis, MO, USA) (35 μ l buffer/10 \times 10⁶ cells). Then, cells were vortexed for 30 s, ice-incubated for 20 min, vortexed for 30 s, and centrifuged in a cool centrifuge for 5 min at 10,000 rpm. After quantification by the Bradford method, lysates were diluted to ≤ 1 mg/ml, when possible, in a mixture of at least 1:2 Novex Tris-glycine SDS sample buffer (2 \times ; Thermo Fisher Scientific) and 2-mercaptoethanol. Lysates were stored at -80°C and boiled 8 min immediately before the array was performed.

Reverse phase protein microarrays

Signal transduction pathway activation was assayed by analysis of the activation/expression of the 51 key signaling proteins shown in **Table 2**.

Antibody validation. Antibodies applicable to RPPA analysis have been extensively validated by single-band specificity on WB. In addition, a Pearson correlation coefficient between RPPA and WB near 0.7 is required. Validation data for Smac/DIABLO, p38 MAPK (Thr-180/Tyr-182), and phospho-*src* family (Tyr-527) were provided from MD Anderson Cancer Center (Houston, TX, USA; please see the "Standard Antibody List" at <https://www.mdanderson.org/education-and-research/resources-for-professionals/scientific-resources/core-facilities-and-services/functional-proteomics-rppa-core/antibody-lists-protocols/functional-proteomics-reverse-phase-protein-array-core-facility-antibody-lists-and-protocols.html>). For the other proteins highlighted in this study, the Pearson correlation validation is shown in **Fig. 1A**.

Printing. Lysates were loaded into a 384-well plate and serially diluted with lysis buffer in 4-point dilution curves ranging from undiluted to 1:8. As positive controls for the antibody staining, we added 3 commercial cell-line lysates: A431, HeLA + pervanadate, NIH3T3-UV treated, and Jurkat cell lysates (BD Biosciences, Franklin Lakes, NJ, USA). Samples were printed in duplicate onto nitrocellulose-coated glass slides (FAST slides, Whatman/Schleicher & Schuell, Florham Park, NJ, USA) with the 2470 Arrayer (Aushon BioSystems, Billerica, MA, USA). Printed slides were desiccated and stored (Drierite; Sigma-Aldrich) at -20°C until use.

Staining. Selected slides were stained with Fast Green FCF (Sigma-Aldrich) according to the manufacturer's instruction to estimate the total protein of each printed sample. Before antibody staining, the arrays were blocked for 1 h at room temperature in blocking solution (2 gr I-Block; Tropix, Bedford, MA, USA and 0.1% Tween-20 in 1 L of PBS 1 \times). Blocked

TABLE 1. Biologic and clinical characteristics of the patients

CLL	WBCs (mm ³)	CD19 ⁺ /5 ⁺ (%)	Mutational status of IGHV	FISH
1	17.800	80	Mutated	13q ⁻
2	67.000	90	Mutated	13q ⁻
3	29.630	87	Mutated	N
4	19.300	89	Mutated	13q ⁻
5	50.200	95	Mutated	N
6	26.700	76	Mutated	Nd
7	22.460	87	Mutated	Nd
8	51.700	95	Mutated	13q ⁻
9	23.900	82	Mutated	Nd
10	19.000	83	Mutated	13q ⁻
11	29.200	88	Mutated	Nd
12	48.000	90	Mutated	Nd
13	108.800	96	Mutated	Nd
14	75.460	89	Mutated	N
15	125.700	88	Mutated	Nd
16	72.620	94	Mutated	Nd
17	21.400	82	Mutated	13q ⁻
18	38.900	88	Mutated	Nd
19	75.500	90	Unmutated	Nd
20	39.900	91	Unmutated	Nd
21	56.000	95	Unmutated	Nd
22	32.000	90	Unmutated	N
23	65.700	66	Unmutated	12 ⁺
24	227.000	98	Unmutated	Nd
25	26.100	96	Unmutated	Nd
26	98.000	76	Unmutated	17p ⁻
27	102.000	98	Unmutated	17p ⁻
28	80.700	94	Unmutated	N
29	259.600	95	Unmutated	Nd
30	31.500	91	Unmutated	13q ⁻
31	148.000	98	Unmutated	11q ⁻ ; 13q ⁻
32	33.900	87	Unmutated	11q ⁻ ; 12 ⁺ ; 13q ⁻
33	65.500	92	Unmutated	N
34	110.200	91	Unmutated	11q ⁻
35	57.500	89	Unmutated	N
36	46.900	90	Unmutated	N
37	16.400	83	Unmutated	Nd
38	45.000	81	Unmutated	Nd
39	10.300	67	Unmutated	11q ⁻ ; 13q ⁻
40	41.100	95	Unmutated	11q ⁻ ; 13q ⁻
41	58.600	93	Unmutated	Nd
42	52.200	93	Unmutated	13q ⁻
43	82.300	74	Unmutated	Nd
44	42.300	88	Unmutated	13q ⁻
45	70.600	97	Unmutated	13q ⁻
46	66.200	97	Unmutated	Nd
47	39.000	95	Mutated	13q ⁻
48	70.000	95	Mutated	Nd
49	37.800	89	Unmutated	Nd
50	29.200	91	Nv	12 ⁺
51	71.430	92	Nv	Nd
52	64.300	82	Nv	17p ⁻ ; 13q ⁻
53	60.400	93	Unmutated	N
54	81.800	93	Unmutated	N
55	19.200	52	Unmutated	11q ⁻ ; 13q ⁻
56	32.600	85	Nv	N
57	20.000	78	Nd	Nd

Mutated was defined as having a frequency of mutations $>2\%$ from the germline VH sequence. N, CLL with a normal karyotype; Nd, not determined; Nv, not valuable.

TABLE 2. Antibodies used for RPPA analysis.

Antibody	Code	Company
Bak	06-536	EMD Millipore
Bax	2772	Cell Signaling
Bcl-2 (S70)	2871/2827	Cell Signaling
Bcl-xL	2762	Cell Signaling
CD45 (35-Z6)	sc-1178	Santa Cruz
CD45 RA	sc-20057	Santa Cruz
CD45 RO (UCH-L1)	sc-1183	Santa Cruz
CDK2 (78B2)	2546	Cell Signaling
Cleaved caspase-6 (Asp-162)	9761	Cell Signaling
Cleaved caspase-7 (Asp-198)	9491	Cell Signaling
Cleaved caspase-9 (Asp-315)	9505	Cell Signaling
Cleaved caspase-9 (Asp-330)	9501	Cell Signaling
Cleaved Notch1 (Val-1744)	2421	Cell Signaling
Cleaved PARP (Asp-214)	9541	Cell Signaling
HDAC6 CT	07-732	EMD Millipore
HS1 (9/HS1)	610540	BD
HSP70 (HSP72)	SPA-810	Enzo
MGMT (MT3.1)	MAB16200	EMD Millipore
Notch1 (6A5)	2495	Cell Signaling
p38 MAPK (Thr-180/Tyr-182)	9211	Cell Signaling
Phospho PKC α (Ser-657)	CI06-822	EMD Millipore
Phospho-Akt (Ser-473)	9271	Cell Signaling
Phospho-CREB (Ser-133)	9191	Cell Signaling
Phospho-FADD (Ser-194)	2781	Cell Signaling
Phospho-FAK (Tyr-397)	611806	BD
Phospho-GSK-3 α/β (Ser-21/9)	9331	Cell Signaling
Phospho-Jak1 (Tyr-1022/1023)	3331	Cell Signaling
Phospho-Lck (Tyr-505)	2751	Cell Signaling
Phospho-MEK1/2 (Ser-217/221)	9121	Cell Signaling
Phospho-mTOR (Ser-2448)	2971	Cell Signaling
Phospho-NF- κ B p65 (Ser-536)	3031	Cell Signaling
Phospho-p44/42 MAPK (Erk1/2) (Thr-202/Tyr-204)	9101	Cell Signaling
Phospho-PDK1 (Ser-241)	3061	Cell Signaling
Phospho-PKC α/β II (Thr-638/641)	9375	Cell Signaling
Phospho-PKC δ (Thr-505)	9374	Cell Signaling
Phospho-PKC δ/θ (Ser-643/676)	9376	Cell Signaling
Phospho-PKC ζ/λ (Thr-410/403)	9378	Cell Signaling
Phospho-SAPK/JNK (Thr-183/Tyr-185)	9251	Cell Signaling
Phospho-SHIP1 (Tyr-1020)	3941	Cell Signaling
Phospho-Smad1 (Ser-463/465)/Smad5 (Ser-463/465)/Smad8 (Ser-426/428)	9511	Cell Signaling
Phospho-Src (Tyr-527)	2105	Cell Signaling
Phospho- <i>src</i> family (Tyr-416)	2101	Cell Signaling
Phospho-Stat1 (Tyr-701)	9171	Cell Signaling
Phospho-Stat3 (Ser-727)	9134	Cell Signaling
Phospho-Stat5 (Tyr-694)	9351	Cell Signaling
SH-PTP1 (D-11)	sc-7289	Santa Cruz
SH-PTP2 (C-18)	sc-280	Santa Cruz
Smac/DIABLO	2954	Cell Signaling
VEGF (A-20)	sc-152	Santa Cruz
ZAP70 (2F3.2)	05-253	EMD Millipore
γ -Tubulin (GTU-88)	T6557	Sigma-Aldrich

BD, BD Biosciences, Franklin Lakes, NJ, USA; Cell Signaling, Cell Signaling Technology, Beverly, MA, USA; EMD Millipore, EMD Millipore, Billerica, MA, USA; Enzo, Enzo Life Sciences, Farmingdale, NY, USA; Santa Cruz, Santa Cruz Biotechnology, Santa Cruz, CA, USA; BD, BD Biosciences, Franklin Lakes, NJ, USA; Sigma-Aldrich, Sigma-Aldrich, St. Louis, MO, USA.

arrays were stained with antibodies on an automated slide stainer (Dako Autostainer Plus; Dako, Carpinteria, CA, USA) using the CSA kit (Dako) as described previously [6]. Slides were air dried and scanned on an Epson (Shinjuku, Tokyo, Japan) Perfection V350 scanner at 600 dpi (dots per inch).

Image analysis. The TIFF (tagged image file format) images of antibody- and Fast Green FCF-stained slides were analyzed with Microvigen Software (VigeneTech Inc, Carlisle, MA, USA) to extract numeric intensity values from the arrays images [7].

Validation. To validate the RPPA data obtained, WB analysis was performed on cells from both patients with CLL and healthy donors, as previously reported [8]. Anti- β -actin mAbs (Sigma-Aldrich) were used as reference proteins. To normalize the phosphoprotein signals, specific antibodies against the total form of the same protein were used. In some cases, results were validated by confocal microscopy, as previously detailed [8].

Confocal microscopy

After 24 h of treatment with 10 μ M dexamethasone (Sigma-Aldrich) to induce apoptosis, cells were collected, washed, plated in polylysine-coated glass for 15 min at room temperature, and fixed in 4% paraformaldehyde for 10 min. The fixed cells were then washed twice with PBS 1 \times and permeabilized with 0.1% Triton X-100 (Sigma-Aldrich) for 4 min. Before staining, nonspecific protein binding was blocked by incubating slides for ≥ 30 min in 2% BSA. Cells were then stained with Smac/DIABLO (Cell Signaling Technology, Danvers, MA, USA) and Tom20 (Santa Cruz Biotechnology, Santa Cruz, CA, USA) for mitochondria staining for ≥ 1 h at room temperature or overnight at 4°C, followed by the secondary antibodies anti-mouse-Alexa488- and anti-rabbit-Alexa594-conjugated, respectively. Background staining with control antibodies was routinely compared with positively stained cells and was not visible using identical acquisition settings. Slides were mounted with cover slips, and fluorescence was detected with the UltraView LCI (PerkinElmer, Waltham, MA, USA) confocal system equipped with a fluorescence filter set for excitation at 488 nm.

Statistical analysis

Statistical analyses after RPPA were performed with R software (R Foundation for Statistical Computing, Wien, Austria). Identification of aberrantly expressed proteins was obtained through Wilcoxon test and *P* values were corrected for multiplicity using the BH method to control the false discovery rate. For other analyses, the Student's *t* test and ANOVA were performed. Data are reported as means \pm sd. *P* < 0.05 was considered significant.

RESULTS AND DISCUSSION

First, we performed an unsupervised clustering analysis, which showed a well-defined separation between patients with CLL and healthy controls (Fig. 1B).

Further investigation of RPPA and the subsequent validation of the results obtained identified molecules whose expression levels reached statistically significant differences in patients with CLL vs. healthy controls. HSP70 and Smac/DIABLO were found to be overexpressed in CLL, whereas the cleaved forms of PARP and caspase-6 were found down-expressed (Fig. 2A and B). The identified molecules are all involved in apoptosis control and could be considered in the design of innovative therapies for CLL. Upon submission of this manuscript, another article by Shull et al. [9] showed an RPPA study in CLL demonstrating alterations of AKT/mTOR-related proteins with eIF4G over-expression and 4E-BP1 Ser-65 phosphorylation contributing to a

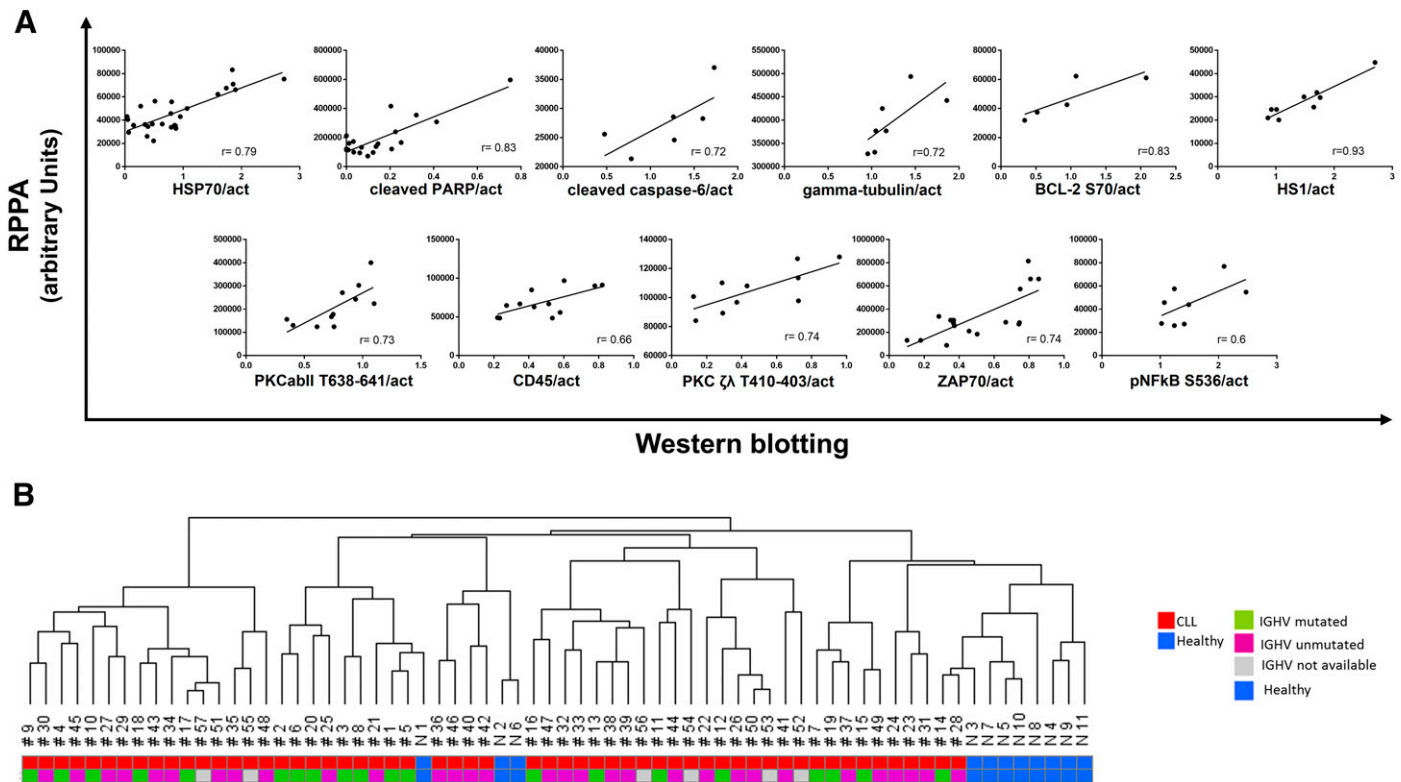


Figure 1. Antibody validation and unsupervised analysis. (A) Pearson correlation coefficient between RPPA and WB for antibody validation. (B) Unsupervised hierarchical clustering analysis of patients with CLL ($n = 57$) and healthy controls ($n = 11$) using Pearson correlation coefficient distance. To place patients in clusters, we used the “complete” method. Color codes identify patient characteristics. #, CLL; N, normal.

CLL prosurvival phenotype. In accordance with that study and, as expected, we found an up-regulation of the prosurvival proteic pattern.

The “molecular machine” HSP70, which inhibits cell death by blocking recruitment of procaspase-9 to the Apaf-1 apoptosome, was found overexpressed in CLL cells (Fig. 2A and B, healthy vs. leukemic B cells; RPPA: $P < 0.01$ Wilcoxon test with BH, validation by WB: $P < 0.01$ Student’s t test). This is not surprising considering that, in CLL, one of the main pathogenetic, intrinsic factors is the lack of an adequate apoptotic response. HSP70 is overexpressed in several tumors and hematologic malignancies, where it is associated with adverse prognostic factors [10]. Moreover, other members of the HSPs (i.e., HSP90 and HSP27) are overexpressed in CLL, indicating a possible role of this family of proteins in the pathogenesis of CLL and, thus, offering the rationale for their use as therapeutic targets.

We also found an overexpression of Smac/DIABLO in patients with CLL with respect to healthy subjects (Fig. 2A and B; healthy vs. leukemic B cells; RPPA: $P < 0.01$ Wilcoxon test with BH, validation by WB: $P < 0.05$ Student’s t test) and a correlation with poor prognosis (Fig. 2C). The extent of Smac/DIABLO expression in cancer cells is controversial. Data from the literature show that, in general, Smac/DIABLO inversely correlates with cancer progression, aggressive behavior, and poor prognosis. In contrast, a direct correlation between Smac/DIABLO expression and cancer progression was reported in

cervical cancer and gastric adenocarcinoma [11, 12]. In the presence of apoptotic stimuli, Smac/DIABLO is normally released from the mitochondria to cytosol, where it provides a proapoptotic effect that is mediated by its antagonization of IAPs. We performed confocal microscopy analysis of Smac/DIABLO in healthy and neoplastic B lymphocytes before and after treatment with the proapoptotic stimulus dexamethasone [13]. Smac/DIABLO was present in the mitochondria of healthy B cells and escaped from them, as expected, when cells were treated. In CLL B cells, Smac/DIABLO was, for the most part, retained in the mitochondria even after treatment, probably unable to carry out its proapoptotic function (Fig. 2D; note merge between Smac/DIABLO and mitochondria in treated CLL B cells). Our preliminary data seem to indicate that the high expression of Smac/DIABLO in CLL cells is restricted to the mitochondria, even after proapoptotic stimulation; notably, there is a lot of Smac/DIABLO, but it does not work properly. We can speculate that, in CLL, HSP70 overexpression inhibits Smac/DIABLO release from the mitochondria and, consequently, the resulting apoptosis, as demonstrated in other cell types [14]. This hypothesis needs to be further validated in CLL, and the detailed mechanisms responsible for the protective effect of HSPs are currently unclear. However, HSP70 may suppress Smac/DIABLO release and apoptosis by up-regulating the expression of the anti-apoptotic protein Bcl2 [14]. Accordingly, we found that Smac/DIABLO directly correlated with Bcl2 phosphorylation at Ser-70 ($P < 0.0001$, Pearson correlation coefficient; Fig. 2E), where

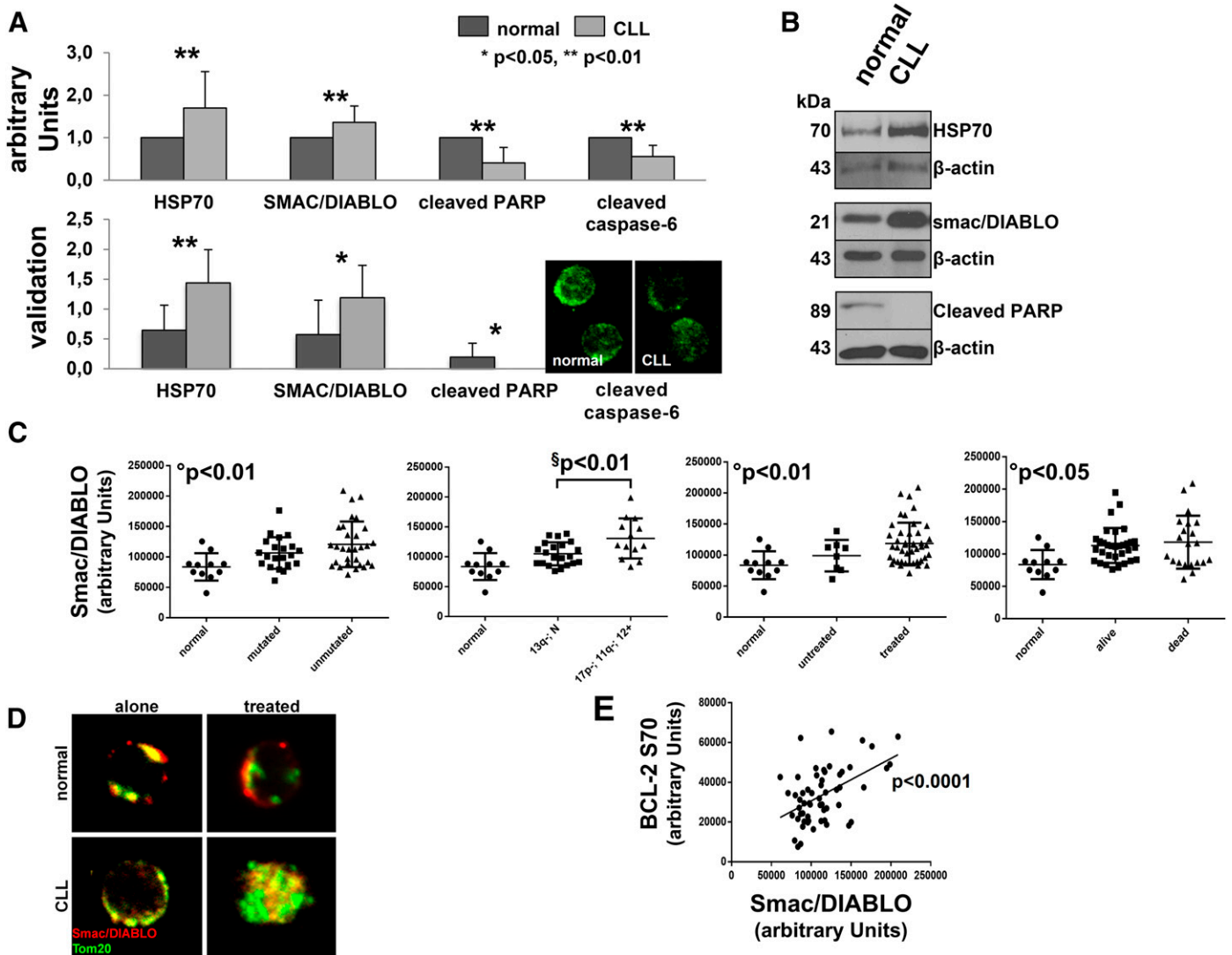


Figure 2. RPPA investigated molecules whose expression levels reached statistically significant differences in patients with CLL vs. healthy controls. (A) Upper histograms represents RPPA values (in arbitrary units) relative to HSP70, Smac/DIABLO, cleaved-PARP, and cleaved caspase-6, which were found to be differentially expressed or activated in CLL vs. healthy B cells ($P < 0.05$ and $**P < 0.01$, Wilcoxon test with BH multiplicity correction); data were normalized, making the means calculated in normal B cells as 1. The lower histograms represent means \pm SD obtained by WB analysis of HSP70/ β -actin, Smac/DIABLO/ β -actin, and cleaved PARP/ β -actin ratios from patients with CLL vs. healthy controls ($*P < 0.05$ and $**P < 0.01$, Student's t test). Image depicts confocal microscopy analysis of cleaved caspase-6 (Alexa488, green). Figure is representative of various experiments (UltraView LCI confocal system, UltraView LCI 5.0 acquisition software; original magnification, $\times 60$). (B) Healthy and leukemic B cells were processed for SDS-PAGE, transferred on nitrocellulose membrane, and revealed with anti-HSP70 and anti- β -actin, anti-Smac/DIABLO and anti- β -actin, anti-cleaved-PARP, and anti- β -actin. (C) RPPA data obtained on Smac/DIABLO expression were evaluated for their prognostic significance with the Student's t Test ($P < 0.01$ between 13q⁻ and normal karyotype CLL vs. 12⁺, 11q⁻, and 17p⁻ CLL) or ANOVA ($P < 0.01$ between normal vs. mutated CLL vs. unmutated CLL and normal vs. treated CLL vs. untreated CLL; $P < 0.05$ normal vs. patients still alive vs. patients who died). Means \pm SD are represented by solid lines ($^{\circ}$ ANOVA, § Student's t test). (D) Confocal microscopy analysis in healthy and CLL B cells of Smac/DIABLO (Alexa488, green) and Tom20 (Alexa594, red) for mitochondria staining. Cells were treated (or not, alone) with 10 μ M of dexamethasone (UltraView LCI confocal system, UltraView LCI 5.0 acquisition software; original magnification, $\times 60$). Yellow, merge. (E) Graph reports the direct correlation between BCL-2 S70 and Smac/DIABLO ($P < 0.0001$ Pearson r correlation). S, serine.

phosphorylation at Ser-70 is a requisite for the strengthening of Bcl2 anti-apoptotic functions.

Caspase-6 is a key caspase known to have both initiator and effector roles in apoptosis by cleavage of caspase-8 and caspase-10 [15]. PARP is found in the nucleus, where it acts as a "sensor" to signal DNA single-strand breaks and to assist in their repair [16]. Caspase-6 and PARP are both cleaved by upstream

caspases into large and small subunits during apoptosis. As demonstrated by RPPA analysis, cl-caspase-6 and cl-PARP are down-regulated in CLL B cells with respect to healthy controls (Fig. 2A and B; healthy vs. leukemic B cells; RPPA: $P < 0.01$ Wilcoxon test with BH, cl-PARP validation by WB: $P < 0.05$ Student's t test), which is not surprising considering that leukemic cells fail to enter the apoptotic process.

Moreover, data from the literature demonstrate a down-regulation of cl-caspase-3 in CLL, and our RPPA analysis also showed a trend of both cl-caspase-7 and cl-caspase-9 down-regulation in leukemic B cells (Fig. 3A and B). Further analysis of these apoptotic players demonstrated that, in patients with CLL, cl-caspase-6 directly correlated with cl-PARP ($P < 0.0001$, Pearson correlation coefficient; Fig. 3C), and the same

correlation was found for cl-caspase-7 vs. cl-caspase-9 ($P < 0.0001$, Pearson correlation coefficient; Fig. 3D). Accordingly, Shull et al. [9] found cl-caspase-7 to be down-regulated in CLL.

Among the proteins mentioned above, which were expressed differently in CLL (HSP70, Smac/DIABLO, cl-caspase-6, and cl-PARP), we focused on the molecular chaperone HSP70, because of its protective role in the cell. Figure 4A represents WB validation of the RPPA results in 42 untreated patients with CLL and 11 healthy subjects. HSP70 was overexpressed in leukemic vs. healthy B cells; in addition, HSP70 expression observed in CLL residual T cells resembled that obtained in healthy B cells, whereas, in the MEC-1 cell line, it was comparable to that found in tumor cells from patients with CLL. Despite the HSP70 mechanisms of action, its over-expression alone may have several implications in CLL. Studies performed on various cancers, including hematologic tumors, have reported a correlation between HSP70 over-expression and therapy resistance [17]. We also analyzed HSP70 levels before and after in vivo treatment, demonstrating a correlation between HSP70 levels and the response to therapy. HSP70, in fact, decreased only in those patients responding to therapy and was unchanged or increased in nonresponding patients and, as a consequence, suggests the involvement of HSP70 in mechanisms of drug resistance (Fig. 4B and C). Cancer cells, which typically express high levels of HSP70, seem to be more dependent on HSP70 than are healthy B cells in terms of survival [18]; inhibitors of the heat shock response may be of particular benefit in the treatment of cancer by breaking that survival advantage that HSP70 gives to cancer cells. HSP70 depletion by antisense oligonucleotides led to the massive death of tumor cells in breast, colorectal, prostate, and liver cancers [19]. For this reason, we tried to inhibit HSP70 in CLL cells with pifithrin- μ , a selective inhibitor of inducible HSP70 reported to affect more cancer than healthy cells by the disruption of the interaction of HSP70 with its cochaperones HSP40 and BAG1 [20]. When tested in our cells, this inhibitor showed significant efficacy in vitro (Fig. 4D). The search for new compounds that lead CLL cells to death is largely justified by the fact that, despite progress made in the treatment of CLL, this malignancy remains an incurable disease for which new approaches are necessary to treat it. With this perspective, we demonstrated that the development of new therapeutic strategies aimed at reducing the HSP70 protective effect could be of interest in the treatment of CLL. It has already been demonstrated in acute and chronic myeloid leukemia that inhibition of HSP70 leads to sensitization of the cells to conventional and new drugs (e.g., etoposide, ara-C, and apoptosis-inducing ligand TNF-derivatives) [21]. Therefore, we investigated the action of pifithrin- μ in the presence of other drugs/molecules (i.e., fludarabine and 17-DMAG). We found that the copresence of pifithrin- μ significantly increased the proapoptotic effect of fludarabine (Fig. 4E), suggesting an involvement of HSP70 in fludarabine-refractory patients. Because data from the literature report that HSP70 inhibition in acute and chronic myeloid leukemia cells increased the antileukemic activity of some derivatives of geldanamycin, we combined pifithrin- μ with 17-DMAG.

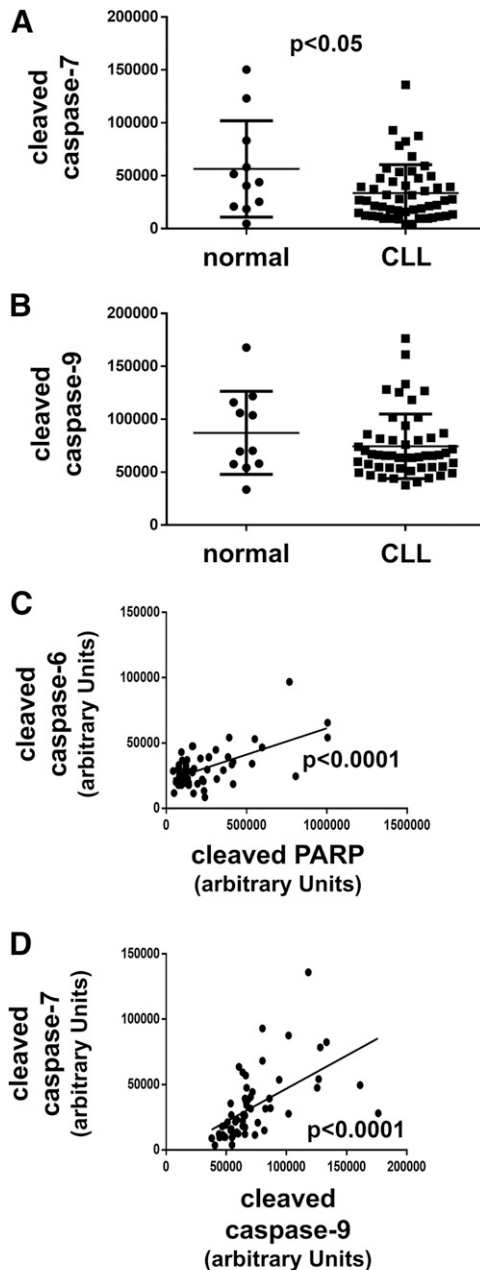


Figure 3. Analysis of cl-caspase-6, cl-caspase-7, cl-caspase-9, and cl-PARP in leukemic B cells. (A) Expression of cleaved caspase-7 in healthy vs. leukemic B cells by RPPA. (B) Expression of cleaved caspase-9 in healthy vs. leukemic B cells by RPPA. (C) Graph reports the direct correlation between cleaved caspase-6 and cleaved PARP ($P < 0.0001$ Pearson r correlation). (D) Graph reports the direct correlation between cleaved caspase-7 and cleaved caspase-9 ($P < 0.0001$ Pearson r correlation).

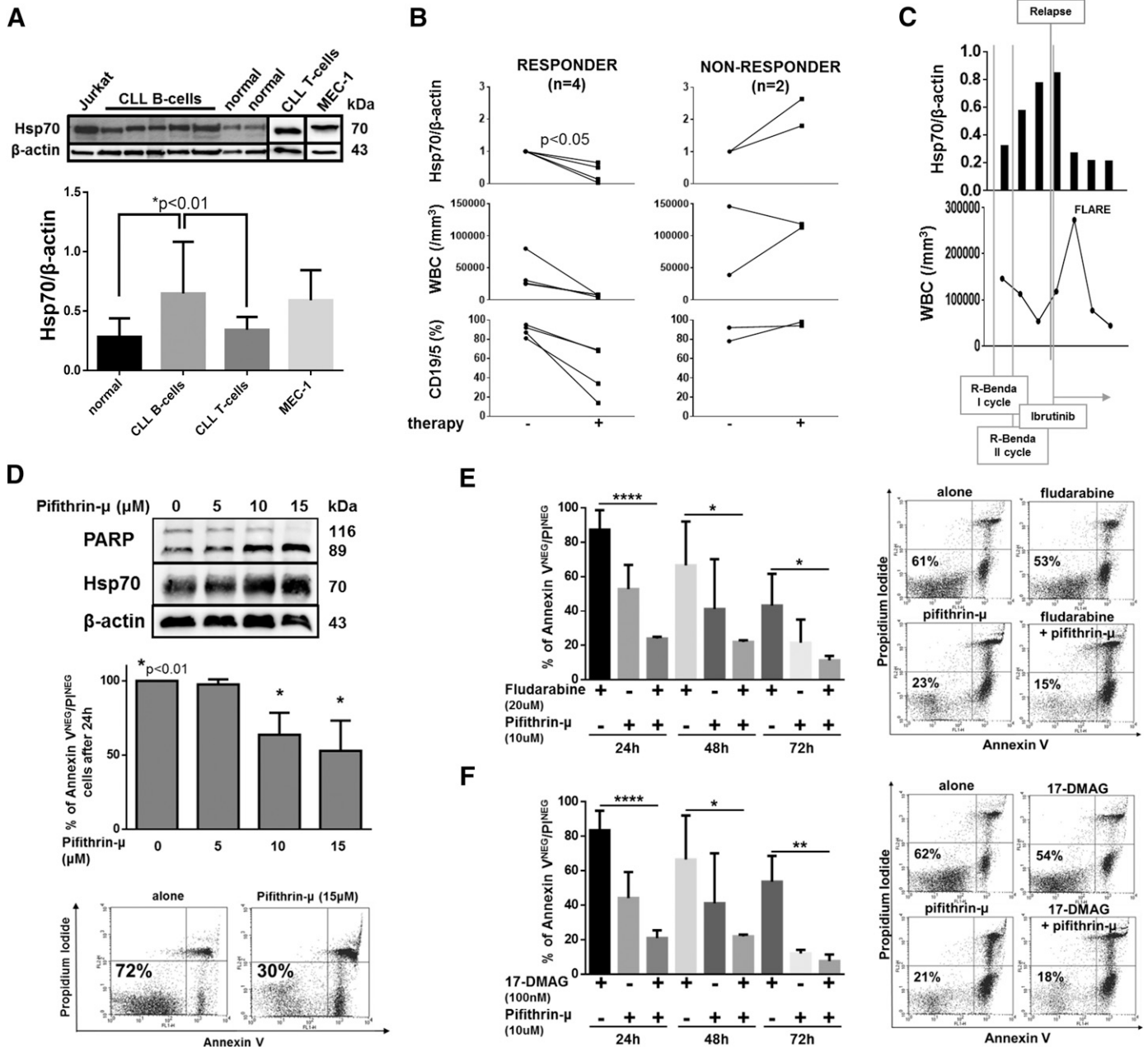


Figure 4. HSP70 characterization in leukemic B cells from patients with CLL. (A) WB analysis was performed in purified B cell samples obtained from untreated patients with CLL ($n = 42$) and healthy subjects ($n = 11$), in residual T cells from CLL ($n = 6$), and in the MEC-1 CLL cell line ($n = 3$). Although there was considerable variation in HSP70 levels in CLL B cells (range, 0.10–1.87), a significant difference in HSP70 expression was observed between malignant B cells from patients (means \pm SD, 0.65 ± 0.43) and B lymphocytes from healthy subjects (0.28 ± 0.15 ; $P < 0.01$, Student's t test). HSP70 expression levels in residual T cells from CLL were 0.23 ± 0.14 and in MEC-1 were 0.59 ± 0.25 . Histograms represent HSP70/β-actin ratio. WB is representative of the cells analyzed. (B) HSP70 expression was analyzed by WB in 6 patients treated with R-FC or R-benda. In particular, the patients examined were as follows: 2 received rituximab, cyclophosphamide, and fludarabine according to the R-FC protocol, which is the gold standard for CLL first-line therapy; and 4 received rituximab and bendamustine (R-benda), which is generally used as second-line therapy. The levels of HSP70 protein were determined in freshly isolated and purified leukemic B cells before (–) and after (+) 1 or 2 cycles of therapy. Figure shows the percentage of HSP70 protein variation by WB after in vivo treatment: 4 of 6 patients showed a reduction in HSP70 after therapy (left column), whereas the others (2 of 6) displayed an increase in the protein (right column). All patients (4 of 6) who showed a reduction in HSP70 after treatment were responsive to therapy (marked reduction in the number of WBCs and CD19⁺/CD5⁺ clonal cells; left). On the contrary, in nonresponding patients (2 of 6; an increase or stability in WBC count and in CD19⁺/CD5⁺ clonal cells, right), we did not observe any reduction, but rather noticed an increase, in HSP70. (C) A CLL case unresponsive to R-benda was followed for several months, and HSP70 expression was correlated to clinical course during therapy. At relapse (WBC/mm³ = 118,410), the patient was initiated to ibrutinib, showing a positive response to

(continued on next page)

This latter compound never achieved CLL clinical trials because its effectiveness was hampered by HSP70 up-regulation. Our results were encouraging because the combination of the 2 molecules significantly increased the ability of 17-DMAG to induce apoptosis in CLL cells (Fig. 4F). Although the regulatory mechanisms of HSPs are not yet entirely clear, this phenomenon can be explained by 17-DMAG being an HSP90 inhibitor acting to inhibit its ATPase activity and, in turn, its cytoprotective function. This inhibitory process destroys the HSP90–HSF1 association, thus promoting nuclear translocation of HSF1 with the resulting up-regulation of HSP70. Because overexpression of HSP70 is considered an important side effect of HSP90 inhibitors (such as 17-DMAG), a combination of HSP90 and HSP70 inhibitors would be desirable to increase the effectiveness of therapy.

RPPA analysis identified another group of proteins that had a trend toward differentiating patients with CLL from healthy controls, with an interesting role in CLL: Hs1, γ -tubulin, PKC- α / β II Thr-638/641, p38 MAPK Thr-180/Tyr-182, NF- κ B Ser-536, Bcl2 Ser-70, and Src Tyr-527 (Fig. 5A and B). Because we and others have already demonstrated that Hs1 is overexpressed in CLL, with prognostic relevance [8, 22], it should be considered for further study as a therapeutic target in this disease. Inhibitors for other proteins studied herein (γ -tubulin, PKC α / β II Thr-638/641, p38 MAPK Thr-180/Tyr-182, NF- κ B Ser-536, and Bcl2 Ser-70), tested in vitro or already entered into clinical practice for the treatment of various diseases, have already been described. Down-regulation of the phosphorylation at the Src inhibitory site (Tyr-527) found in CLL cells (Fig. 5B) is interesting because Lyn is the most prominent SFK expressed and activated in CLL B cells [13]. The antibody to the inhibitory site of Src, indeed, cross-reacts with other members of the SFKs when phosphorylated at equivalent sites. If the electrophoretic bands obtained by the WB immunostaining (53 of 56 instead of 60 kDa; Fig. 5B) correspond to the molecular weight of Lyn, its constitutive phosphorylation/up-regulation at the activator site in CLL cells is consistent with the finding of down-regulation of the inhibitory Src/Lyn site.

CLL cases can have somatically mutated, as well as unmutated, IGHV genes, which largely correlate with a favorable and unfavorable clinical prognosis, respectively [1, 3]. Although the unsupervised clustering analysis did not

distinguish IGHV mutated vs. unmutated cases in our study or in Shull *et al* [9], when we analyzed single proteins, we found that ZAP70 and PKC- ζ Thr-410/403 were overexpressed in patients with unmutated cells, whereas CD45 was overexpressed in patients with mutated cells (Fig. 5C and D). Among all proteins, the protein kinase ZAP70 has emerged from this type of analysis. In fact, its expression in leukemic B cells was already associated [23] with an aggressive course of the disease, allowing for more-effective IgM signaling, a feature that could contribute to the relatively aggressive clinical behavior generally associated with unmutated IGHV status. CLL B cell response to surface IgM is, in fact, generally greater in unmutated cases, with ZAP70 and CD38 expression enhancing signal competence [24]. ZAP70 is usually detected by flow cytometry, providing conflicting results [25]. Conversely, our RPPA validation was obtained by WB analysis, corroborating the early studies on ZAP70 expression [23] and raising, once again, the question of whether flow cytometry is the most suitable method for the analysis of this protein, considering that this technique has led to variable results among different laboratories.

In conclusion, this study identified some new molecules that are differently expressed in CLL vs. healthy B cells, as well as in mutated vs. unmutated cells, which could be considered an opening for further studies, in view of their clinical, prognostic, and pathogenic relevance in CLL. Of special interest will be those deregulated molecules that are implicated in apoptosis control. In particular, the results obtained in this study highlight the role of HSP70 in the survival of CLL cells and the efficacy of its inhibitors in inducing apoptosis in leukemic clones, suggesting that, in the future, HSP70 could become an attractive therapeutic target for the development of new therapeutic strategies, alone or in combination, for CLL.

AUTHORSHIP

F.F., B.A., and L.T. conceived and designed the experiments. B.A., G.M., S.B., and G.B. performed the RPPA analysis. F.F., V.T., C.G., V.M., F.S., and A.V. performed the experiments for RPPA validation. F.F. and B.A. analyzed and interpreted the data. G.S. and L.T. contributed clinical patient samples. F.F., B.A., and L.T. wrote the article. G.B., G.S., and L.T. provided intellectual input into the study and reviewed the manuscript.

treatment demonstrated by a progressive decrease in the WBC count (the observed transient elevation in WBC count fell within the phenomenon of “flare,” typical of the response to this drug). Response to ibrutinib corresponded to a decrease in HSP70 expression levels. (D) CLL B cells were cultured alone or in the presence of 5, 10, and 15 μ M pifithrin- μ , and cell apoptosis was analyzed by the Annexin V/PI flow cytometric test. Histograms show the percentage of Annexin V⁺/PI⁺ cells after 24 h of treatment. Data are reported as means \pm SD and were normalized, 100% equal to the means \pm SD calculated in the untreated patients (* P < 0.01 between untreated [alone, 0] vs. pifithrin- μ treatment at 10 μ M and 15 μ M; paired Student's t test). Cytochrome of the annexin V/PI test related to a representative case are reported. In all conditions, the total cell lysates were subjected to SDS/PAGE, transferred to a nitrocellulose membrane and were detected sequentially with anti-PARP to highlight the apoptosis, anti-HSP70, and anti- β -actin. Figure shows a representative case. (E) Experiments were performed, and data are reported as in D. In this case, we used pifithrin- μ (10 μ M), fludarabine (20 μ M), and their combinations (pifithrin- μ + fludarabine) for 24, 48, and 72 h. In particular, percentages of viable cells (means \pm SD) at the different timing were as follows: **** P < 0.0001 between fludarabine alone vs. pifithrin- μ + fludarabine at 24 h, * P < 0.05 between fludarabine alone vs. pifithrin- μ + fludarabine at 48 h and 72 h (Student's t test). (F) Experiments were performed, and data are reported as in D. In this case, we used pifithrin- μ (10 μ M), 17-DMAG (100 nM), and their combinations (pifithrin- μ + 17-DMAG) for 24, 48, and 72 h (**** P < 0.0001 between 17-DMAG alone vs. pifithrin- μ + 17-DMAG at 24 h, * P < 0.05 between 17-DMAG alone vs. pifithrin- μ + 17-DMAG at 48 h, ** P < 0.001 between 17-DMAG alone vs. pifithrin- μ + 17-DMAG at 72 h; Student's t Test). Cytochrome of annexin V/PI test related to a representative case are reported. Percentages reported in the cytochrome represent viable annexin V^{neg}/PI^{neg} cells. CLL, chronic lymphocytic leukemia; PI, propidium iodide.

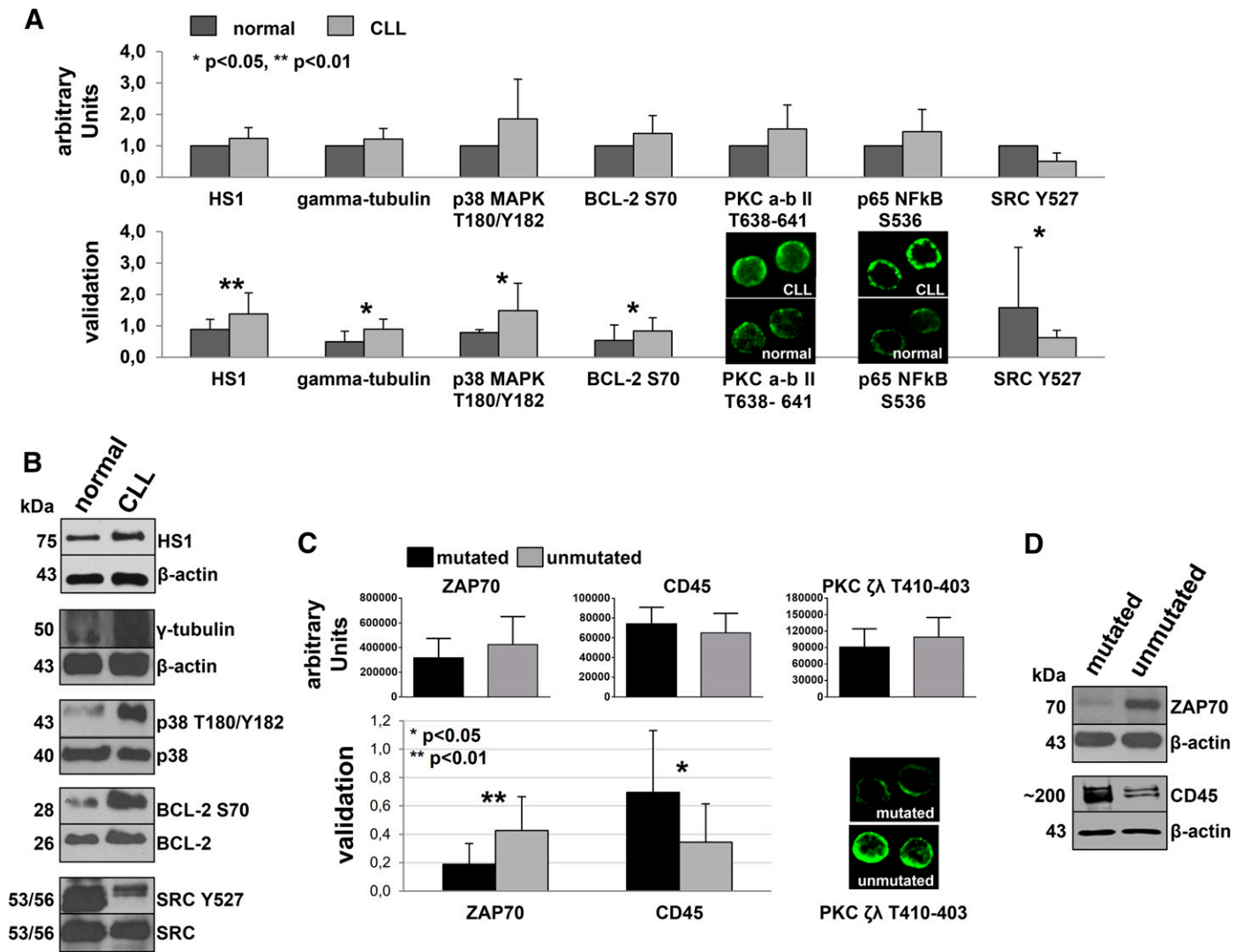


Figure 5. RPPA investigated molecules with a positive trend of difference in patients with CLL vs. healthy controls. (A) Upper histograms represents RPPA values (arbitrary units) relative to HS1, γ -tubulin, p38MAPK T180/Y182, Bcl-2 S70, PKC-a-b II T638-641, p65 NF- κ B S536, and Src Y527, which were found to be differentially expressed or activated in CLL vs. healthy B cells (Wilcoxon test); data were normalized, making the means calculated in healthy B cells equal to 1. Lower histograms represent means \pm SE obtained by WB analysis of HS1/ β -actin, γ -tubulin/ β -actin, p38MAPK T180/Y182/p38MAPK, Bcl-2 S70/Bcl-2, and Src Y527/Src from patients with CLL vs. healthy controls ($*P < 0.05$ and $**P < 0.01$, Student's *t* test). Images depict confocal microscopy analysis of PKC a-b II T638-641 and p65 NF- κ B S536 (Alexa488, green). Figures are representative of various experiments (UltraView LCI confocal system, UltraView LCI 5.0 acquisition software; original magnification, $\times 60$). (B) Healthy and leukemic B cells were processed for SDS-PAGE, transferred on nitrocellulose membranes, and treated with anti-HS1 and anti- β -actin, anti- γ -tubulin and anti- β -actin, anti-p38MAPK T180/Y182 and anti-p38MAPK, anti-Bcl-2 S70 and anti-Bcl-2, and anti-Src Y527 and anti-Src. (C) Upper histograms represent RPPA values (arbitrary units) relative to ZAP70, CD45, and PKC- ζ T410-403, found to be differentially expressed in mutated vs. unmutated CLL (Wilcoxon test). Lower histograms represent means \pm SD obtained by WB analysis of ZAP70/ β -actin and CD45/ β -actin ratios of mutated vs. unmutated cells from patients with CLL vs. healthy controls ($*P < 0.05$ and $**P < 0.01$, Student's *t* test). Images depict confocal microscopy analysis of PKC-a-b II T638-641 and p65 NF- κ B S536 (Alexa488, green). Figures are representative of various experiments (UltraView LCI confocal system, UltraView LCI 5.0 acquisition software; original magnification, $\times 60$). (D) CLL B cells from patients with either mutated or unmutated cells were processed for SDS-PAGE, transferred on nitrocellulose membranes, and treated with anti-ZAP70 and anti- β -actin and anti-CD45 and anti- β -actin. S, serine; T, threonine; Y, tyrosine.

ACKNOWLEDGMENTS

This work was supported by funds from Ministero dell'Istruzione dell'Università e della Ricerca (PRIN 2008, 2010–2011, to L.T., FIRB 2010 to G.S.), Associazione Italiana per la Ricerca sul Cancro (AIRC project#15397 to L.T.), Fondazione CARIPARO-Progetto Pediatria to G.B., and AIRC regional

project with Fondazione Cariparo and Cariverona, Regione Veneto on Chronic Lymphocytic Leukemia. F.S. has a fellowship from AIRC (15397).

DISCLOSURES

The authors declare no competing financial interests.

REFERENCES

1. Stevenson, F. K., Krysov, S., Davies, A. J., Steele, A. J., Packham, G. (2011) B-cell receptor signaling in chronic lymphocytic leukemia. *Blood* **118**, 4313–4320.
2. Zenz, T., Mertens, D., Küppers, R., Döhner, H., Stilgenbauer, S. (2010) From pathogenesis to treatment of chronic lymphocytic leukaemia. *Nat. Rev. Cancer* **10**, 37–50.
3. Hamblin, T. J., Davis, Z., Gardiner, A., Oscier, D. G., Stevenson, F. K. (1999) Unmutated Ig V(H) genes are associated with a more aggressive form of chronic lymphocytic leukemia. *Blood* **94**, 1848–1854.
4. Liotta, L. A., Espina, V., Mehta, A. I., Calvert, V., Rosenblatt, K., Geho, D., Munson, P. J., Young, L., Wulfschuh, J., Petricoin III, E. F. (2003) Protein microarrays: meeting analytical challenges for clinical applications. *Cancer Cell* **3**, 317–325.
5. Danilov, A. V. (2013) Targeted therapy in chronic lymphocytic leukemia: past, present, and future. *Clin. Ther.* **35**, 1258–1270.
6. Wulfschuh, J. D., Aquino, J. A., Calvert, V. S., Fishman, D. A., Coukos, G., Liotta, L. A., Petricoin III, E. F. (2003) Signal pathway profiling of ovarian cancer from human tissue specimens using reverse-phase protein microarrays. *Proteomics* **3**, 2085–2090.
7. Accordi, B., Espina, V., Giordan, M., VanMeter, A., Milani, G., Galla, L., Ruzzene, M., Sciro, M., Trentin, L., De Maria, R., te Kronnie, G., Petricoin, E., Liotta, L., Basso, G. (2010) Functional protein network activation mapping reveals new potential molecular drug targets for poor prognosis pediatric BCP-ALL. *PLoS One* **5**, e13552.
8. Frezzato, F., Gattazzo, C., Martini, V., Trimarco, V., Teramo, A., Carraro, S., Cabrelle, A., Ave, E., Facco, M., Zambello, R., Tibaldi, E., Brunati, A. M., Semenzato, G., Trentin, L. (2012) HS1, a Lyn kinase substrate, is abnormally expressed in B-chronic lymphocytic leukemia and correlates with response to fludarabine-based regimen. *PLoS One* **7**, e39902.
9. Shull, A. Y., Noonepalle, S. K., Awan, F. T., Liu, J., Pei, L., Bollag, R. J., Salman, H., Ding, Z., Shi, H. (2015) RPPA-based protein profiling reveals eIF4G overexpression and 4E-BP1 serine 65 phosphorylation as molecular events that correspond with a pro-survival phenotype in chronic lymphocytic leukemia. *Oncotarget* **6**, 14632–14645.
10. Thomas, X., Campos, L., Mounier, C., Cornillon, J., Flandrin, P., Le, Q. H., Piselli, S., Guyotat, D. (2005) Expression of heat-shock proteins is associated with major adverse prognostic factors in acute myeloid leukemia. *Leuk. Res.* **29**, 1049–1058.
11. Arellano-Llamas, A., Garcia, F. J., Perez, D., Cantu, D., Espinosa, M., De la Garza, J. G., Maldonado, V., Melendez-Zajgla, J. (2006) High Smac/DIABLO expression is associated with early local recurrence of cervical cancer. *BMC Cancer* **6**, 256.
12. Shibata, T., Mahotka, C., Wethkamp, N., Heikau, S., Gabbert, H. E., Ramp, U. (2007) Disturbed expression of the apoptosis regulators XIAP, XAF1, and Smac/DIABLO in gastric adenocarcinomas. *Diagn. Mol. Pathol.* **16**, 1–8.
13. Contri, A., Brunati, A. M., Trentin, L., Cabrelle, A., Miorin, M., Cesaro, L., Pinna, L. A., Zambello, R., Semenzato, G., Donella-Deana, A. (2005) Chronic lymphocytic leukemia B cells contain anomalous Lyn tyrosine kinase, a putative contribution to defective apoptosis. *J. Clin. Invest.* **115**, 369–378.
14. Jiang, B., Liang, P., Deng, G., Tu, Z., Liu, M., Xiao, X. (2011) Increased stability of Bcl-2 in HSP70-mediated protection against apoptosis induced by oxidative stress. *Cell Stress Chaperones* **16**, 143–152.
15. Slee, E. A., Harte, M. T., Kluck, R. M., Wolf, B. B., Casiano, C. A., Newmeyer, D. D., Wang, H. G., Reed, J. C., Nicholson, D. W., Alnemri, E. S., Green, D. R., Martin, S. J. (1999) Ordering the cytochrome c-initiated caspase cascade: hierarchical activation of caspases-2, -3, -6, -7, -8, and -10 in a caspase-9-dependent manner. *J. Cell Biol.* **144**, 281–292.
16. de Murcia, G., Ménissier de Murcia, J. (1994) Poly(ADP-ribose) polymerase: a molecular nick-sensor. *Trends Biochem. Sci.* **19**, 172–176.
17. Ciocca, D. R., Calderwood, S. K. (2005) Heat shock proteins in cancer: diagnostic, prognostic, predictive, and treatment implications. *Cell Stress Chaperones* **10**, 86–103.
18. Lanneau, D., Brunet, M., Frisan, E., Solary, E., Fontenay, M., Garrido, C. (2008) Heat shock proteins: essential proteins for apoptosis regulation. *J. Cell. Mol. Med.* **12**, 743–761.
19. Nylandsted, J., Brand, K., Jäättelä, M. (2000) Heat shock protein 70 is required for the survival of cancer cells. *Ann. N. Y. Acad. Sci.* **926**, 122–125.
20. Leu, J. I., Pimkina, J., Frank, A., Murphy, M. E., George, D. L. (2009) A small molecule inhibitor of inducible heat shock protein 70. *Mol. Cell* **36**, 15–27.
21. Guo, F., Sigua, C., Bali, P., George, P., Fiskus, W., Scuto, A., Annavarapu, S., Mouttaki, A., Sondarva, G., Wei, S., Wu, J., Djeu, J., Bhalla, K. (2005) Mechanistic role of heat shock protein 70 in Bcr-Abl-mediated resistance to apoptosis in human acute leukemia cells. *Blood* **105**, 1246–1255.
22. Scielzo, C., Ghia, P., Conti, A., Bachi, A., Guida, G., Geuna, M., Alessio, M., Caligaris-Cappio, F. (2005) HS1 protein is differentially expressed in chronic lymphocytic leukemia patient subsets with good or poor prognoses. *J. Clin. Invest.* **115**, 1644–1650.
23. Crespo, M., Bosch, F., Villamor, N., Bellosillo, B., Colomer, D., Rozman, M., Marcé, S., López-Guillermo, A., Campo, E., Montserrat, E. (2003) ZAP-70 expression as a surrogate for immunoglobulin-variable-region mutations in chronic lymphocytic leukemia. *N. Engl. J. Med.* **348**, 1764–1775.
24. Mockridge, C. I., Potter, K. N., Wheatley, I., Neville, L. A., Packham, G., Stevenson, F. K. (2007) Reversible anergy of sIgM-mediated signaling in the two subsets of CLL defined by VH-gene mutational status. *Blood* **109**, 4424–4431.
25. Degheidy, H. A., Venzon, D. J., Farooqui, M. Z., Abbasi, F., Arthur, D. C., Wilson, W. H., Wiestner, A., Stetler-Stevenson, M. A., Marti, G. E. (2011) Methodological comparison of two anti-ZAP-70 antibodies. *Cytometry B Clin. Cytom.* **80B**, 300–308.

KEY WORDS:

signal transduction · lymphocyte · HSP70 · Smac/DIABLO